Spin-polarized transport in a quasi-1D wire with Rashba dots

Dae Han Park, Heesang Kim, Youngsin Park [iD], and Nammee Kim [iD]

View Online   Export Citation   CrossMark

ARTICLES YOU MAY BE INTERESTED IN

Spin-polarized transport in a quasi-1D wire with Rashba dots

Dae Han Park,[1] Heesang Kim,[1] Youngsin Park,[2] and Nammee Kim[1,a]

[1]*Department of Physics, Soongsil University, Seoul 06978, Korea*
[2]*School of Natural Science, Ulsan National Institute of Science and Technology (UNIST), Ulsan 44919, Korea*

A numerical study on spin-polarized transport properties in a quasi-one-dimensional wire with Rashba quantum dots is presented. The ballistic spin transmission probability and spin density profiles are obtained using the quantum transmitting boundary method. The Fano-Rashba effect on the spin transmission is analyzed as a function of the Rashba spin-orbit coupling strength for single dot and double dot systems. The spin density profiles show the localized states that contribute to the backscattering and spin-flip processes in the Rashba dots. The results enlighten us on the Fano-Rashba effect caused by local Rashba spin-orbit coupling and provide concrete ideas for modeling a system with spin-polarized transport for future applications. © *2018 Author(s).*

I. INTRODUCTION

The development of nanotechnology has been a subject of significant focus in recent decades. Fundamental studies have been carried out on the properties of materials and the possibility of a new paradigm of applications. As part of this effort, research involving the spin degree of freedom of the electron has recently exploded.

Magnetic fields can be used as a tool to manipulate the direction of spin of an electron. The spins of electrons naturally align along the direction of the magnetic field. This has led to studies of many different materials, such as ferromagnetic metals and diluted magnetic semiconductors. But from the perspective of applications, it is much more convenient to control the direction of spin using only an electric field and not a magnetic field. One method of doing this is the Rashba effect. After the Datta-Das-type spin transistor[1] was proposed, the Rashba effect, first reported in the 1960s, attracted renewed attention because it plays a crucial role in manipulating spins in spintronic devices. In various InAs quantum well structures, the spin band splitting has a magnitude of several meV and the Rashba coupling parameter is of the order of 10^{-11} eV m. The intrinsic Rashba effect in a semiconductor hetero-structure caused by the asymmetric potential is small when the asymmetric potential is small. However, the asymmetric potential can be tuned using an additional electric field external to the system.[2,3] In a spin transistor, electrons with aligned spins are injected into the channel and an external electric field induces strong Rashba spin-orbit coupling (RSOC) to rotate the spins. This is the key concept behind a spin-polarized field effect transistor (SPFET).

The ballistic conductance of a two-dimensional electron gas (2DEG) system has been a subject of study for many years. Recently, the transport properties of a one-dimensional quantum wire (1DQW) have been investigated extensively, since only a few populated sub-bands are allowed in the 1DQW compared to the 2DEG system.[4,5] The 2DEG system has many propagating channels, because the Rashba-induced spin-splitting is comparable to the energy sub-band spacing. Therefore,

---

[a]Email: nammee@ssu.ac.kr

the ballistic conductance of 1DQWs based on semiconductors, metals, and other compound materials has been studied with or without external magnetic fields in various ways in the search for possible applications.[6–14]

The Fano effect is a quantum interference effect that occurs when a discrete energy level and continuum energy states are present in the same system. The electrons traveling through the continuum energy states are trapped in discrete energy level states. This effect has been widely studied in an interferometer with quantum dots.[15–17] When the dots are formed by RSOC, it is called the Fano-Rashba effect.

In this paper, we numerically study spin-dependent transmission in a 1DQW with various numbers of Rashba quantum dots. An area of local RSOC controlled by electrical gating is called an embedded Rashba quantum dot (RQD). We choose the one dimensional system to avoid mixing effect between propagating channels. The aim of this work is to propose a spin device based on RSOC and to investigate how the Fano-Rashba effect changes with the number of RQDs. Because we focus on the spin precession due to RSOC only, we do not include an external magnetic field. A quasi-one-dimensional wire (Q1DW) formed by applying split gates to a 2DEG system has well-separated channels. While most previous works have considered uniform RSOC throughout the channel[6–12] or a local RSOC in small energy range,[13,14] we consider various numbers of local RSOC in a large range of energy in order to study the Fano effect as a function of the number of local RSOC. With a modulation of the local RSOC, we study the Rashba-Fano effect as well as the spin-polarized transmission in the system. Alongside changing the strength of the local RSOC, we analyze the Fano-Rashba effect in the double dot case and compare it to the single dot case. With a clearer understanding of the Fano effect, the result of this study give more concrete ideas controlling the spin polarization of the output current, which would contribute to the spin filter and the spin transistor modeling. These numerical studies can be further extended to study physical properties of a system having two dimensional semiconductor materials like a graphene and a transition metal dichalcogenide as a channel material.[18–21]

We show a schematic diagram of our model systems in Fig. 1. The scattering region is sandwiched between two leads. Although the spin injection rate associated with the resistivity mismatch between the lead and the channel is an important issue in spintronics research, the material of the lead is not relevant in our numerical calculations. If a 2DEG formed by semiconductor hetero-structures is considered, diluted ferromagnetic semiconductor (DMS) leads are preferred to increase the spin injection rate in the experiment. The DMS leads require a low temperature experimental environment.
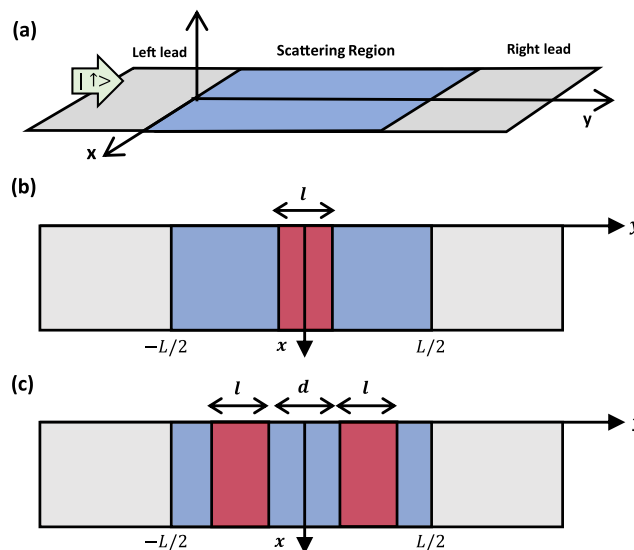

FIG. 1. (a) A schematic diagram of a quasi-1D quantum wire with a parabolic confinement potential along the x-axis. The spin direction of incident electrons is fixed to | ↑> along the z-axis. (b) A quantum wire with a single Rashba dot of size l. (c) A quantum wire with double Rashba dots, each of size l, with a distance between the two of d.

We impose a parabolic confinement potential along the x-axis to induce electron movement along the y-axis. Since the movement along the x-axis is limited, we call this system a quasi-1D wire. The parabolic confinement potential can be created using the additional electrostatic potential of additional split gates in the 2DEG system. The diagrams for the one and two RQD cases are shown in Figs. 1(b) and 1(c). We focus on the dependence of the observed effects on the number of dots. In our model, the intrinsic RSOC due to the inversion asymmetry, which is often treated as a perturbed term in analytical calculations, is considered negligible compared to the RSOC created by the external electric field.

II. THEORY

The effective mass Hamiltonian of a Q1DW with RQDs can be written as follows:

$$H = \frac{\hbar^2}{2m^*}\left(\frac{\partial^2}{\partial x^2} + \frac{\partial^2}{\partial y^2}\right) + \frac{1}{2}m^*\omega_c^2 x^2 + H_R,$$ (1)

where $\frac{1}{2}m^*\omega_c^2 x^2$ is the confinement potential along the x-axis and $H_R = \frac{1}{2\hbar}(\{\alpha(y), p_y\}\sigma_x - \{\alpha(y), p_x\}\sigma_y)$ is the RSOC-Hamiltonian. The confinement potential gives transverse modes $\epsilon_n = \hbar\omega_c(n - \frac{1}{2})$ ($n = 1, 2, \ldots$). Here, $\{\}$ represents an anti-commutator, α is the Rashba strength, and $\sigma_i(i = x, y, z)$ is the Pauli matrix.

Since most previous works have considered uniform RSOC throughout the channel of the system, they have used a constant Rashba strength α. However, we use α as a function of space to allow for local RSOC. When α is a function of space, $H_R = \frac{\alpha}{\hbar}(\vec{\sigma} \times \vec{p})$ is not Hermitian and the Rashba Hamiltonian must be defined using an anti-commutator to ensure the hermiticity of the Hamiltonian.[15] After including Pauli matrices, the Hamiltonian in the dimensionless form $\tilde{H}$ becomes

$$\tilde{H} = \begin{pmatrix} -\left(\partial_x^2 + \partial_y^2\right) + x^2 & -i\gamma(y)\partial_y + \gamma(y)\partial_x - i\frac{1}{2}(\partial_y\gamma(y)) \\ -i\gamma(y)\partial_y - \gamma(y)\partial_x - i\frac{1}{2}(\partial_y\gamma(y)) & -\left(\partial_x^2 + \partial_y^2\right) + x^2 \end{pmatrix},$$ (2)

where the unit energy is $\frac{1}{2}\hbar\omega_c$ and the unit length l_0 is $\sqrt{\frac{\hbar}{m\omega_c}}$. When we choose the unit of energy to be 10 meV, the unit of length is about 10 nm. The function $\gamma(y)$ is a dimensionless Rashba strength defined as a function of space as $\gamma(y) = \gamma_0\left(f\left(y - \frac{l}{2}\right) - f\left(y + \frac{l}{2}\right)\right)$ for a single RQD[15] (Fig. 1(b)) and $\gamma(y) = \gamma_0(f(y - \frac{3}{2}l - \frac{1}{2}d) - f(y - \frac{1}{2}l - \frac{1}{2}d) + f(y + \frac{1}{2}l + \frac{1}{2}d) - f(y + \frac{3}{2}l + \frac{1}{2}d))$ for double RQDs (Fig. 1(c)) with $f(y) = 1/(1 + e^{y/\sigma})$. Here, d is the distance between the RQDs, γ_0 is the strength of the RSOC, and σ is a small diffusivity. Since the physical dimension of α is energy times length, we calculate the dimensionless constant as $\gamma_0 = \frac{2m\alpha_0}{\hbar^2}l_0 = \frac{\alpha_0}{0.5\hbar\omega_c \times l_0}$. The Rashba coupling parameter α_0 is related to the gate electric field linearly. The dimensionless constant γ_0 is also proportional to the gate electric field and represents the strength of RSOC in the dots.

The wave functions of incident electrons in the nth mode in the left and right leads are written as,[22,23]

$$\Psi_{L,n}(x, y) = e^{ik_n y}\psi_{\uparrow n}(x)|\uparrow> + \sum_{j=1}^{\infty}\left(r_{j,\uparrow\uparrow}e^{-ik_j y}\psi_{\uparrow,j}(x)\big|\uparrow> + r_{j,\uparrow\downarrow}e^{-ik_j y}\psi_{\downarrow,j}(x)\big|\downarrow>\right),$$ (3)

$$\Psi_{R,n}(x, y) = \sum_{j=1}^{\infty}\left(t_{j,\uparrow\uparrow}e^{ik_j y}\psi_{\uparrow,j}(x)\big|\uparrow> + t_{j,\uparrow\downarrow}e^{ik_j y}\psi_{\downarrow,j}(x)\big|\downarrow>\right),$$ (4)

where $k_n = \sqrt{E_F - \varepsilon_n}$, E_F is the Fermi energy, and $\varepsilon_n(= \hbar\omega_c(n - 1/2))$ is the nth eigen-energy for a parabolic confinement potential along the x-axis. $r_{j,\uparrow\uparrow}$ and $t_{j,\uparrow\uparrow}$ correspond to the reflection and transmission coefficients, respectively, of the jth sub-band for a spin-up state to a spin-up state. Evanescent modes ($\varepsilon_n > E_F$) decay exponentially outside the scattering region. By using the wave function in the scattering region, $\Psi_S(x, y) = \phi_{\uparrow}(x, y)|\uparrow> + \phi_{\downarrow}(x, y)|\downarrow>$, the transmission probabilities (TP) for a spin-up state to a spin-up state in the nth sub-band and the jth sub-band are calculated as follows:[24]

$$T_{n,j,\uparrow\uparrow} = \frac{f_{tran}}{f_{inc}} = \frac{k_j}{k_n}\left|t_{j,\uparrow\uparrow}\right|^2,$$ (5)

where f_{inc} and f_{tran} are the probability flux incident and transmitted, respectively. When we consider propagation along the same sub-band only, $T_{n,n,\uparrow\uparrow} = \left| t_{j,\uparrow\uparrow} \right|^2$. In the scattering region, the spin density of the spin-up state is defined as

$$\rho_\uparrow(x,y) = |<\uparrow|\Psi_S(x,y)>|^2 = |\phi_\uparrow(x,y)|^2. \tag{6}$$

The $T_{n,j,\uparrow\downarrow}$ and the spin density $\rho_\downarrow(x,y)$ for the spin-down case are written similarly to Eqs. (5) and (6).

As we all know, the analytical solution of this system is very difficult to obtain. Therefore, we perform numerical calculations based on the Quantum Transmitting Boundary Method (QTBM) developed by C. S. Lent.[25] The QTBM is written in the frame of the finite element method, which is one of the numerical approaches used to solve partial differential equations. The QTBM can be applied to a system with an arbitrary potential and several leads. 5041 nodal points are assigned to each spin component in our calculation.

III. RESULTS AND DISCUSSION

The electrons do not really share a single direction except when they pass through a magnet. However, to study how the localized RSOC changes the direction of spin, we assume that the injected electrons are aligned in one direction. We consider a case in which spin-up (+z-direction) electrons are injected into our numerical calculation. We show the TP as a function of the Fermi energy (E_F) for different numbers of quantum dots and different RSCO strengths (γ_0) in Fig. 2. In our calculation, propagation in the lowest sub-band (n=1) is considered and we write $T_{1,1,\uparrow\uparrow}$ simply as $T_{\uparrow\uparrow}$ hereafter. We analyze the results from two perspectives – that of the TP rate change and that of the Fano-Rashba resonance (FRR) dip change upon variation of the number of dots and the RSOC strength (γ_0). While the ballistic TP in a wire with uniform RSOC has a constant value of 1, an FRR dip and a total TP of less than 1 appear in the wire with the local RSOC. From the calculation, we see that the depth of the FRR dip changes drastically as γ_0 changes. The FRR dip starts to appear around $\gamma_0 = 0.8$. As γ_0 increases, the dip width becomes larger and the dip moves to lower energy both in the single dot and double dot cases. A notable result arises in the rate of spin inversion for the two different cases. In the double RQD case, the spins of the incident electrons are flipped even in the low energy region. There is almost no spin-up transmission where $E_F < 1.0$ (the dotted line in Fig. 2(d)). However, in the same energy region, the spin inversion occurs partially in the single RQD case and there are both spin-up and spin-down transmissions (Fig. 2(b)). This result shows that the double RQD is more efficient in generating spin-polarized electrons in transmission. For $\gamma_0 = 2.0$, the total TP is significantly reduced due to backscattering, resulting in a smaller output signal than $\gamma_0 = 1.0$ in both the single and double
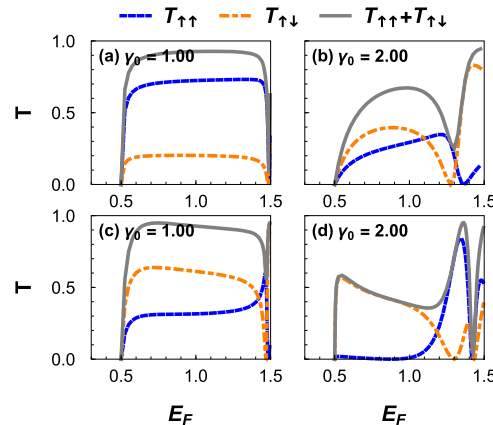

FIG. 2. The transmission probabilities $T_{\uparrow\uparrow}$ (dotted line), $T_{\uparrow\downarrow}$ (dash-dotted line), and $T_{\uparrow\uparrow} + T_{\uparrow\downarrow}$ (solid line) with different Rashba strengths γ_0. (a) $\gamma_0 = 1.00$ and (b) $\gamma_0 = 2.00$ for the single Rashba dot case. (c) $\gamma_0 = 1.00$ and (d) $\gamma_0 = 2.00$ for the double Rashba dot case. All parameters are in dimensionless units.

dot cases. We will come back to this point again, when we discuss Fig. 4. When we consider the case of spin-down (- z-direction) electrons being injected, we have the results that $T_{\downarrow\uparrow} = T_{\uparrow\downarrow}$ and $T_{\downarrow\downarrow} = T_{\uparrow\uparrow}$. We present all the results in dimensionless units. If the unit of energy is 10 meV and the unit of length is about 10 nm, $\gamma_0 = 2.0$ is of the order of 10^{-12} eV m and the Rashba spin splitting energy is much smaller than the sub-band energy splitting of the parabolic confinement energy.[6] The ballistic transport through the lowest sub-band is a reasonable approximation and the parameters we use in the numerical calculation are realistic.

To understand the FRR dip, we plot the spin density profile for the double RQD system in Fig. 3. We plot two cases for comparison. One is a case with $\gamma_0 = 1.0$ and $E_F = 0.6$, which corresponds to the case in Fig. 2(c). This point has total TP value close to 1.0. The other is a case with $\gamma_0 = 2.0$ and $E_F = 1.4$, which is a position where FRR occurs in Fig. 2(d). In the former case, the up-spins of incident electrons start to rotate to down-spins in the region of the first RQD. The regions of the dots are drawn as shaded areas in each figure. As a result, the spin-down density is dominant at the end of the wire as shown in Fig. 3(b). The spin precession depends on the length of a dot and on the strength of RSOC. In our case, the spin rotates by π for $\gamma_0 = 1.0$ and by 2π for $\gamma_0 = 2.0$. In the latter case of $\gamma_0 = 2.0$ for E_F near the FRR dip, there exist localized states at the dot region. They contribute to the backscattering in both the spin-up and spin-down cases, resulting in a reduction of the TP as shown in Fig. 3(c) (spin-up) and in Fig. 3(d) (spin-down). Both the spin-up and spin-down electrons are localized at the two RQDs. While the density profile in the single dot case takes a dicotyledon form,[25] that in the double dot case looks like a four-leaf clover.

As we noticed that the double RQDs produce well-defined spin-polarization as shown in Fig. 2(d), we now focus on the transmission of the double RQD system in detail. We show the spin-up and the spin-down TPs as a function of the Rashba strength γ_0 and the Fermi energy E_F in Fig. 4. Note that spin-up electrons are injected into the system in this case. In the small $\gamma_0 < 0.5$ region, the spin-up transmission is dominant in all through the E_F region (Figs. 4(a) and (b)). In the region where $\gamma_0 > 0.5$, the spin precession due to the Rashba effect being prominent means spin-up and the spin-down transmission coexist. As E_F goes up, each TP oscillates with γ_0 variation. When $E_F > 1.3$ and $\gamma_0 > 2.0$, we notice that there appears a Fano-Rashba resonance line where the total
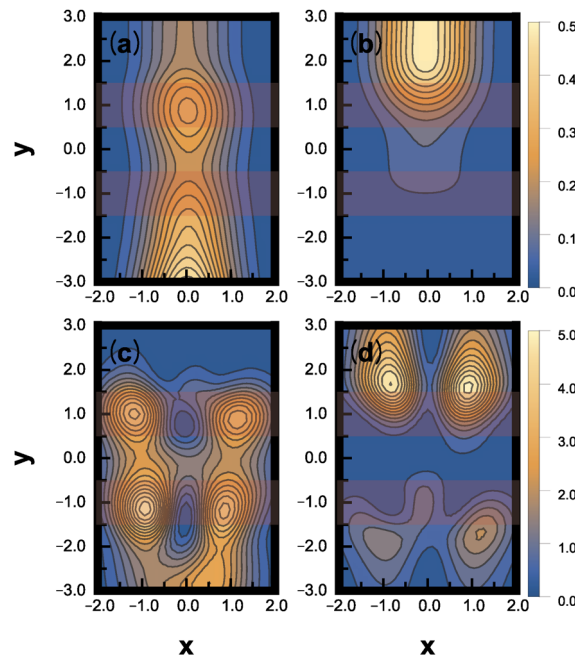

FIG. 3. Spin density profiles for a wire with double Rashba dots. (a) Spin-up and (b) spin-down density profiles with Rashba strength $\gamma_0 = 1.00$ and Fermi energy $E_F = 0.6$. (c) Spin-up and (d) spin-down density profiles with $\gamma_0 = 2.00$ and $E_F = 1.42$. All parameters are in dimensionless units.
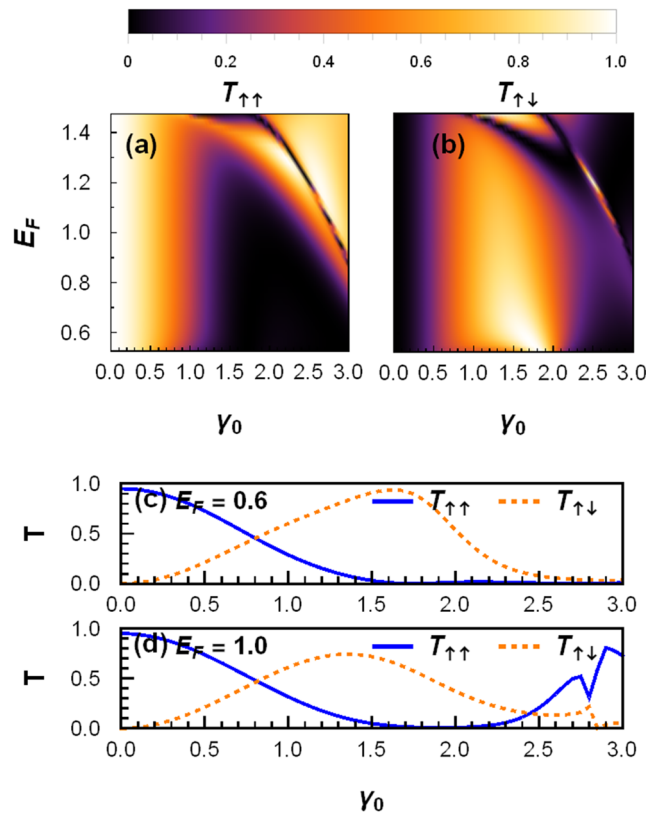
FIG. 4. The transmission probabilities for the double Rashba dot case ($l = 1$, $d = 1$). (a) $T_{\uparrow\uparrow}$ and (b) $T_{\uparrow\downarrow}$ are obtained as a function of the Rashba strength γ_0 and the Fermi energy E_f simultaneously. (c) The transmission probabilities $T_{\uparrow\uparrow}$ (solid line) and $T_{\uparrow\downarrow}$ (dotted line) as a function of the Rashba strength γ_0 for a fixed Fermi energy $E_f = 0.6$. (d) As (c), but for $E_f = 1.0$. All parameters are in dimensionless units.

TP becomes zero. Note that in the present setting, the transmission is through the lowest energy sub-band. We know that spin conductance changes with the energy of incident electrons from previous figures. Here, to show the manipulation of the spin-polarization by changing γ_0, we plot the spin-up and spin-down TPs as a function of the Rashba strength γ_0. For $E_F = 0.6$ (Fig. 4(c)), when $\gamma_0 > 1.5$, only the spin-down electrons can travel to the end of the channel in our plot range. In this case, the spin-up polarized current cannot be obtained by varying γ_0. For $E_F = 1.0$ (Fig. 4(d)), however, we can get either a spin-down or spin-up current by choosing $\gamma_0 = 1.5$ or $\gamma_0 = 3.0$. This means that the spin-polarization can be manipulated electrically. Of course, the backscattering mentioned above reduces the total output current. This phenomenon seems intrinsic to a wire with localized RSOC.

IV. CONCLUSION

We have investigated the Fano-Rashba effect for ballistic spin-polarized transmission through a quasi-1D semiconductor quantum wire with different numbers of Rashba quantum dots. The Fano-Rashba resonance dip shifts to lower energies and the dip width becomes wider as the Rashba spin-orbit coupling strength increases in both the single and double dot cases. The Fano-Rashba effect is well explained by the spin density profiles of the localized states, which are responsible for backscattering. The spin precession caused by the Rashba quantum dots induces a change in the transmission probability. A double dot system is more effective at producing the polarized spin current than a single dot system. This polarization of the spin current can be manipulated by an external electric field, which produces the local Rashba spin-orbit coupling. Since the total transmission probability is suppressed by localized states in Rashba dots, the value of the local Rashba spin-orbit coupling

strength should be chosen carefully when designing a spin device using Rashba quantum dots to optimize signal detection.

ACKNOWLEDGMENTS

[1] S. Datta and B. Das, Appl. Phys. Lett. **56**, 665 (1990).
[2] J. Nitta, T. Akazaki, H. Takayanagi, and T. Enoki, Phys. Rev. Lett. **78**, 1335 (1997).
[3] D. Grundler, Phys. Rev. Lett. **84**, 6074 (2000).
[4] P. R. Hammer, B. R. Bennett, M. J. Yang, and M. Johnson, Phys. Rev. Lett. **83**, 203 (1999); J. App. Phys. **87**, 4665 (2000).
[5] S. Gardelis, C. G. Smith, C. H. W. Barnes, E. H. Linfield, and D. A. Ritchie, Phys. Rev. B **60**, 7764 (1999).
[6] F. Mireles and G. Kirczenow, Phys. Rev. B **64**, 024426 (2001).
[7] Y. V. Pershin, J. A. Nesteroff, and V. Privman, Phys. Rev. B **69**, 121306 (2004).
[8] L. Serra, D. Sánchez, and R. Lopez, Phys. Rev. B **72**, 235309 (2005).
[9] S. J. Gong and Z. Q. Yang, J. Appl. Phys. **102**, 033706 (2007).
[10] X. Xiao, Z. Chen, W. Nie, G. Zhou, and F. Li, J. Appl. Phys. **115**, 223709 (2014).
[11] M. R. Sakr, Physica E **81**, 253 (2016).
[12] N. Pournaghavi, M. Esmaeilzadeh, A. Abrishamifar, and S. Ahmadi, J. Phys.: Condens. Matter **29**, 145501 (2017).
[13] L. Chirolli, D. Venturelli, F. Taddei, R. Fazio, and V. Giovannetti, Phys. Rev. B **85**, 155317 (2012).
[14] A. F. Sadreev and E. Ya. Sherman, Phys. Rev. B **88**, 115302 (2013).
[15] D. Sánchez and L. Serra, Phys. Rev. B **74** 153313 (2006); J. Phys.: Conf. Ser. **61**, 1037 (2007).
[16] P. A. Orellana, M. Amado, and F. Domínguez-Adame, Nanotechnology **19**, 195401 (2008).
[17] M. L. Vallejo, M. L. L. de Guevara, and P. A. Orellana, Phys. Lett. A **374**, 4928 (2010).
[18] A. Mreńca-Kolasińska, B. Rzeszotarski, and B. Szafran, Phys. Rev. B **98**, 045406 (2018).
[19] M. Inglot, V. K. Dugaev, E. Ya. Sherman, and J. Barnaś, Phys. Rev. B **91**, 195428 (2015).
[20] Kh. Shakouri, M. Ramezani Masir, A. Jellal, E. B. Choubabi, and F. M. Peeters, Phys. Rev. B **88**, 115408 (2013).
[21] D. Rainis and D. Loss, Phys. Rev. B **90**, 235415 (2014).
[22] H. Xie, F. Jiang, E. Wei, and I. Sha, Comput. Phys. Commun. **108**, 118 (2016).
[23] L. Serra and D. Sanchez, *Progress in Industrial Mathematics at ECMI 2006* (2008), Vol. 12, p. 449.
[24] L. Ramdas Ram-Mohan, *Finite Element and Boundary Element Applications in Quantum Mechanics*, 2002, p. 482.
[25] C. S. Lent and D. J. Krikner, J. Appl. Phys. **67**, 6353 (1990).